

## Effect of deposition temperature on thermal stability in high-density plasma chemical vapor deposition fluorine-doped silicon dioxide

Y. L. Cheng, Y. L. Wang, H. W. Chen, J. L. Lan, C. P. Liu, S. A. Wu, Y. L. Wu, K. Y. Lo, and M. S. Feng

Citation: *Journal of Vacuum Science & Technology A* **22**, 494 (2004); doi: 10.1116/1.1690779

View online: <http://dx.doi.org/10.1116/1.1690779>

View Table of Contents: <http://scitation.aip.org/content/avs/journal/jvsta/22/3?ver=pdfcov>

Published by the AVS: Science & Technology of Materials, Interfaces, and Processing

---

### Articles you may be interested in

Methods of producing plasma enhanced chemical vapor deposition silicon nitride thin films with high compressive and tensile stress

*J. Vac. Sci. Technol. A* **26**, 517 (2008); 10.1116/1.2906259

Effects of thermal annealing on the structural, mechanical, and tribological properties of hard fluorinated carbon films deposited by plasma enhanced chemical vapor deposition

*J. Vac. Sci. Technol. A* **22**, 2321 (2004); 10.1116/1.1795833

Effect of fluorine incorporation on silicon dioxide prepared by high density plasma chemical vapor deposition with SiH<sub>4</sub> O<sub>2</sub> NF<sub>3</sub> chemistry

*J. Appl. Phys.* **96**, 1435 (2004); 10.1063/1.1767979

Thermal stability enhancement of Cu/WN/SiOF/Si multilayers by post-plasma treatment of fluorine-doped silicon dioxide

*J. Appl. Phys.* **85**, 473 (1999); 10.1063/1.369410

Structure of fluorine-doped silicon oxide films deposited by plasma-enhanced chemical vapor deposition

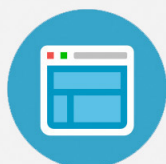
*J. Vac. Sci. Technol. A* **15**, 2908 (1997); 10.1116/1.580884

---



## Re-register for Table of Content Alerts

Create a profile.



Sign up today!



# Effect of deposition temperature on thermal stability in high-density plasma chemical vapor deposition fluorine-doped silicon dioxide

Y. L. Cheng

*Department of Material Science and Engineering, National Chiao-Tung University, Hsin-Chu, Taiwan, Republic of China*

Y. L. Wang,<sup>a)</sup> H. W. Chen, and J. L. Lan

*Taiwan Semiconductor Manufacturing Company, Ltd., Hsinchu, Taiwan, Republic of China*

C. P. Liu

*Department of Material Science Engineering, National Cheng-Kung University, Tanani, Taiwan, Republic of China*

S. A. Wu

*Taiwan Semiconductor Manufacturing Company, Ltd., Hsinchu, Taiwan, Republic of China*

Y. L. Wu

*Department of Electrical Engineering, National Chi-Nan University, Nan-Tou, Taiwan, Republic of China*

K. Y. Lo

*Department of Applied Physics, National Chiayi-University, Chiayi, Taiwan, Republic of China*

M. S. Feng

*Department of Material Science and Engineering, National Chiao-Tung University, Hsin-Chu, Taiwan, Republic of China*

(Received 26 June 2003; accepted 2 February 2004; published 14 April 2004)

Thermal stability of fluorine-doped silicon dioxide films deposited by high-density plasma chemical vapor deposition as a function of deposition temperature were investigated in this study. Both thermal desorption spectrum and annealing test results show that SiOF films deposited above 400 °C have better thermal stability. Furnace annealing data indicate that non —Si—F— bonding fluorine does exist in low-deposition-temperature SiOF films. Furthermore, secondary-ion mass spectrometer results also reveal that the fluorine in SiOF films with a lower-deposition temperature is easily diffused out and turned into the underlayer, which results in less thermally stable SiOF films. Moreover, short-loop simulation results have been subsequently tested and it was concluded that the deposition temperature of the SiOF film is extremely important for thermal stability.

© 2004 American Vacuum Society. [DOI: 10.1116/1.1690779]

## I. INTRODUCTION

With recent progress of high integration and modern ultralarge-scale integration achieving gate widths of less than 0.25  $\mu\text{m}$ , it has become necessary to further improve device operating speed, which is limited by the capacitance of inter-metal dielectric (IMD) capacitance. To reduce the IMD capacitance, fluorine-doped silicon dioxide (SiOF)<sup>1</sup> films deposited by high-density plasma chemical vapor deposition (HDP-CVD) have been introduced in an advanced IMD application. The HDP-CVD technique has been demonstrated to have good gap-filling capability and film stability.<sup>2,3</sup> Moreover, in 1998, Yang *et al.*<sup>4</sup> produced SiOF films in 0.18  $\mu\text{m}$  logic devices. As a consequence, SiOF films are considered a suitable and a manufacturable low dielectric constant (low- $k$ ) IMD for devices below 0.25  $\mu\text{m}$ .

Many researchers have studied the formation process of SiOF films, viewing it as having a low  $k$ , excellent gap-filling ability due to *in situ* etching by SiF<sub>4</sub>, and being void free. They point out that the higher fluorine concentration

would lower the dielectric constant<sup>5–8</sup> and improve the gap-filling ability. However, these researchers also express caution that SiOF films have a thermal stability issue that affects the integration. The subsequent deposition of a SiOF-capped silicon-dioxide (SiO<sub>2</sub>), metal film, and passivation layer has shown blistering after the alloying process.<sup>9</sup> As a result, precursors, reaction methods, and optimized process conditions have been proposed to improve the thermal stability of SiOF films.<sup>10–13</sup>

In this work, we conducted a comprehensive study of the dependence on the deposition temperature of the physical properties and thermal stability of SiOF films prepared by HDP-CVD using Ar, O<sub>2</sub>, SiH<sub>4</sub>, and SiF<sub>4</sub> gas. The relevance of the deposition temperature in influencing the properties of SiOF films is reported. Also, a comparative analysis of thermal desorption spectrum (TDS), annealing test, and secondary-ion mass spectrometer (SIMS) results allow us to determine the thermal stability of individual SiOF films with varying deposition temperature.

<sup>a)</sup>Also at: Department of Electrical Engineering, National Chi-Nan University, Nan-Tou, Taiwan, Republic of China.

TABLE I. Property of SiOF film trends at 350–450 °C-deposition temperature.

	Deposition rate	Fluorine concentration at. % F	Dielectric constant	Refractive index	Stress	Wet etch rate	Hardness
Deposition temperature	↑	↓	↓	↑	↑	↑	↑

## II. EXPERIMENT

The SiOF films were prepared in an Ultima HDP-CVD Applied Materials Centura 5200 system using Ar/O<sub>2</sub>/SiH<sub>4</sub>/SiF<sub>4</sub> as reaction gas. The gas flow rate of Ar, O<sub>2</sub>, SiH<sub>4</sub>, and SiF<sub>4</sub> were 50, 110, 45, and 30 cm<sup>3</sup>/min, respectively. The deposition temperature was detected at the back side of the deposited wafer by a wafer temperature monitor. The back side He pressure was adjusted to control the deposition temperature, which we varied from 350 to 450 °C. The as-deposited films were analyzed for thickness and refractive index (RI, at 633 nm) by reflectometry and/or ellipsometry using the Nano-Spec 9100. This thickness of the SiO film is the net-deposition (ND) thickness under rf bias conditions, which is the sum of deposition, sputter, and etch. The sputter (*S*) rate was measured by sputtering the SiOF films for 60 s on a blanket wafer using Ar gas. The pure deposition (PD) thickness (no sputter/no etch effects) was determined by setting the bias rf to zero on a blanket wafer. Therefore, the removal thickness due to sputter and etch (*S+E*) effects should be the PD thickness minus the ND thickness. The etch (*E*) rate was then calculated by subtracting the thickness of *S* from the removal thickness of sputter and etch (*S+E*). TDS and furnace alloy samples were deposited directly on bare silicon wafers. In addition, SIMS was used to analyze the film structure based on a silicon wafer that was first covered with a SiO<sub>2</sub> film, then a SiOF film of different temperatures, and then capped with a SiO<sub>2</sub> layer.

The furnace annealing condition reached 425 °C for 60 min in nitrogen ambients and the alloying process required seven heating/cooling cycles in total. Next, the fluorine concentration was measured before and after alloying by infrared (IR) spectroscopy using a Bio-rad Fourier transform instrument, using the Si—F band at about 930 cm<sup>-1</sup> and also using x-ray fluorescence (XRF). We quantified the Si—F/Si—O peak-height ratios in the reflectance mode. The IR analysis was performed at a resolution of 4 cm<sup>-1</sup>, averaging 16 scans. XRF detected F bonded in both Si—F and non—Si—F— configurations in 200 second scans. The SiOF films with different deposition temperatures were prepared, and then the gap-filling capability of the various SiOF films was determined by scanning electron microscopy (SEM). Subsequently, the structure of short-loop samples was simulated on a 0.18 μm IMD scheme, to verify and support previous TDS and alloying results.

## III. RESULTS AND DISCUSSIONS

### A. Film property

Figure 1 shows the refractive index of SiOF thin films,

measured by ellipometry, as a function of the SiOF deposition temperature. For these films deposited by HDP-CVD, the refractive indices are 1.40–1.45, which are lower than the 1.46 value of thermal oxide SiO<sub>2</sub>. It is well known that the refraction index is closely related to the porosity of these SiO<sub>2</sub>-based materials, being smaller for higher porosity. Therefore, porosity might be one reason for the lower refractive indices. However, as shown in Fig. 1, the RI decreases appreciably with decreasing SiOF film deposition temperature, but with increasing fluorine content. This shows that the lower RI may also be influenced by fluorine incorporation into SiO<sub>2</sub>. Further support for this may be found with the IR spectra. We find that at lower deposition temperature, the peak of the Si—O stretching band shifts to a higher frequency, in the presence of a high concentration of fluorine in the structure. As a consequence, the Si—O—Si bond angle opens up slightly, resulting in a cage structure (porosity) in the film. This structure causes the density of the film to decrease. Therefore, the RI also decreases with decreasing deposition temperature. Agreeing with this result, the dielectric constant of the as-deposited SiOF film decreases to 3.346 at 350 °C from 3.964 at 450 °C. The reduction of electronic polarization by more Si—F bonds and by an increment in porosity in the SiOF film, both contribute to a lower *k*. Table I summarizes the trends for increasing deposition temperatures. The deposition rate increases as the SiOF deposition temperature decreases owing to fluorine having less thermal energy in which to provide plasma etching. For higher-deposition temperatures, the SiOF film becomes denser as a result of the plasma etching ability to remove weak bonds, and results in a material having lower wet etch rates. It is worth noticing that the hardness of the SiOF films decreases as the deposition temperature decreases due to an increase in porosity and decrease in cross linking due to reactor incor-

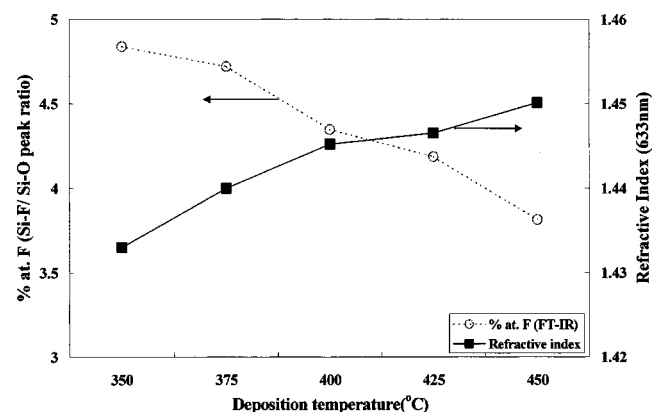


FIG. 1. Effect of deposition temperature on the concentration of fluorine and refractive index for SiOF film.

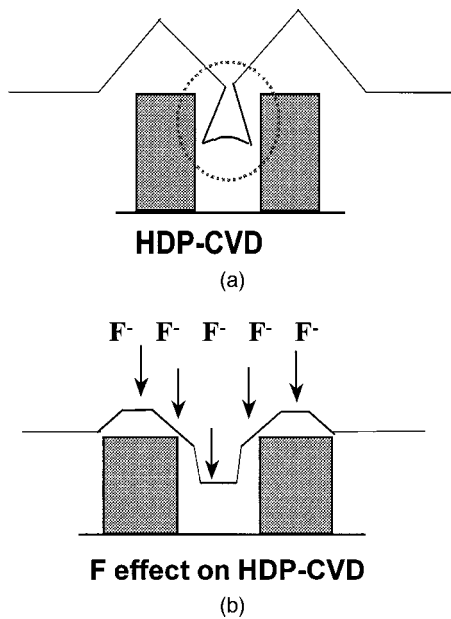


FIG. 2. Concept of HDP-CVD gap filling: (a) HDP-CVD and (b) F-doped HDP-CVD.

poration of terminal Si—F bonds. The hardness of the low- $k$  film is an essential property during processing with chemical mechanical polishing (CMP).

### B. Gap-filling ability

As the minimum geometry of integrated-circuit devices becomes increasingly smaller, the separation between metal lines becomes smaller, as well. Because the deposition rate is lower at the side wall of the metal gaps than at the bottom of the gap, HDP-CVD has been introduced to enhance the gap-filling ability owing to the sputter ability of high-density plasma. However, it still has difficulties in filling higher-aspect ratio gaps, without voids [Fig. 2(a)]. On the other hand, we can use the etching ability of fluorine to facilitate the deposition to fill the smaller gap [Fig. 2(b)]. Therefore, to investigate the effect of deposition temperature on the gap-filling ability, we separated the HDP-CVD SiOF deposition process into three main reactions: Deposition ( $D$ ), sputter ( $S$ ), and etch ( $E$ ). Furthermore, we also defined the parameter  $D/(S+E)$  as the gap-filling index. The better the gap-filling capability, the smaller the  $D/(S+E)$  value. The calculated results are summarized in Table II. As seen in Table II, the  $E/(S+E)$  value quantifies the contribution of the etch

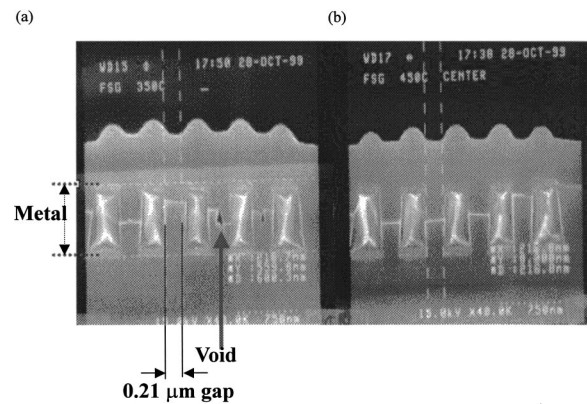


FIG. 3. SEM image of SiOF film for checking gap filling (height/gap =  $0.6 \mu\text{m}/0.21 \mu\text{m}$ ): (Left-hand side)  $350^\circ\text{C}$ , (right-hand side)  $450^\circ\text{C}$ .

component of the total removal in the HDP-CVD SiOF process, and this value increases with the rise of deposition temperature. The result also shows that the sputter rate is temperature independent in our experimental temperature range. Thus, the etch rate contribution to the total removal rate increases with temperature. There is about a 5% increase in etch rate with an increase of  $100^\circ\text{C}$  temperature, which causes a decrease of the  $D/(S+E)$  ratio. Therefore, we infer that SiOF films with a higher deposition temperature prepared by HDP-CVD should have a high gap-filling capacity compared to those with a lower deposition temperature.

The gap-filling ability was investigated by depositing SiOF films with different deposition temperatures wafers patterned with different metal widths/gaps. Figure 3 reveals that a  $350^\circ\text{C}$ -deposited SiOF film can fill into the metal gap with  $0.25 \mu\text{m}$  spacing, but not reach the void-free requirement for a  $0.21 \mu\text{m}$  gap [Fig. 3(a)]. On the other hand, a higher deposition temperature ( $\sim 450^\circ\text{C}$ ) can fill a  $0.21 \mu\text{m}$  metal gap (aspect ratio was 3.6) with no metal clipping, which implies that the etch ability of the F atom has increased abruptly at the higher temperature on the wafer. Again, we also demonstrate that the deposition rate decreases with increased deposition temperature due to the fact that F etches  $\text{SiO}_2$  more effectively at high temperature.

### C. Thermal stability-outgassing issues

In real interconnect fabrication, thermal treatment is an indispensable step. Here, the interconnect medium consists of up to eight separate layers, all of which are deposited at

TABLE II. Effect of deposition temperature on gap-filling parameters of SiOF process.

Deposition temperature (°C)	Deposition rate $D$ (Å/min)	Sputter rate $S$ (Å/min)	Etch rate $E$ (Å/min)	$E/(S+E)$	$E/S$	$D/(S+E)$	$D/S$	$D/E$	$E/S$
350	3607	1541	1011	0.396	0.656	1.374	2.341	3.568	0.656
375	3553	1548	1028	0.399	0.656	1.340	2.295	3.456	0.664
400	3506	1553	1067	0.407	0.687	1.300	2.258	3.286	0.687
425	3480	1538	1080	0.412	0.702	1.291	2.263	3.223	0.702
450	3393	1542	1112	0.419	0.721	1.241	2.200	3.052	0.721

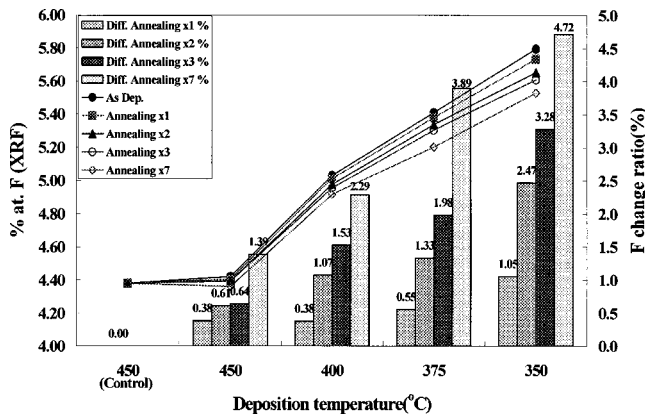


Fig. 4. Difference of XRF of SiOF films with varying deposition temperature.

about 400 °C. As a result, a suitable interconnect dielectric should possess excellent thermal resistance. To study the thermal stability of SiOF films with varying deposition temperature, the films were annealed in N<sub>2</sub> ambient for 1 h at 425 °C. The film thickness, RI, and fluorine concentration (IR value) after annealing all remained stable even after repeated annealing tests (seven times) through the entire range of deposition temperatures. This points out that the Si—O and Si—F bonds in SiOF films have enough thermal resistance against a 425 °C heat treatment. However, the fluorine content measured by XRF gradually declined and reached saturation after the third annealing test. Moreover, the magnitude of this decline is dependent upon the deposition temperature of SiOF films. The SiOF film with a lower-deposition temperature has a larger change in XRF value, as shown in Fig. 4. IR was used to monitor the Si—F/Si—O ratio, calibrated with Rutherford backscattering, and XRF detected total fluorine content (including bonding Si—F and non—Si—F— bonding fluorine). Consequently, we can use Eq. (1) to calculate the amount of non —Si—F— bonding:

$$\text{XRF/IR} = 1 + (\text{non—Si—F—})/\text{Si—F}. \quad (1)$$

The higher XRF/IR ratio means a higher amount of non —Si—F— bonding fluorine. As shown in Fig. 5, the lower deposition temperature of the SiOF process has more non —Si—F— bonding fluorine. This can explain the result of Fig. 4. As the SiOF film with a lower-deposition temperature was immersed into a N<sub>2</sub> ambient at an elevated temperature, more non —Si—F— bonding fluorine outgassed in the thermal process. Furthermore, after three cycles of the annealing process, for the SiOF film with a deposition temperature above 400 °C, the outgassing reached saturation. On the contrary, the fluorine at.% (XRF value) kept decreasing for SiOF films with deposition temperatures below 400 °C, even after seven cycles of the annealing process. This implies that SiOF films deposited at temperatures lower than 400 °C have greater amounts of either weak Si—F bonding or nonbonded fluorine (free fluorine). Hence, the weaker Si—F units will be broken, or free fluorine will be outgassed by the thermal process. Considering this outgas as excess fluorine, this excess could possibly be avoided by the use of a lower gas

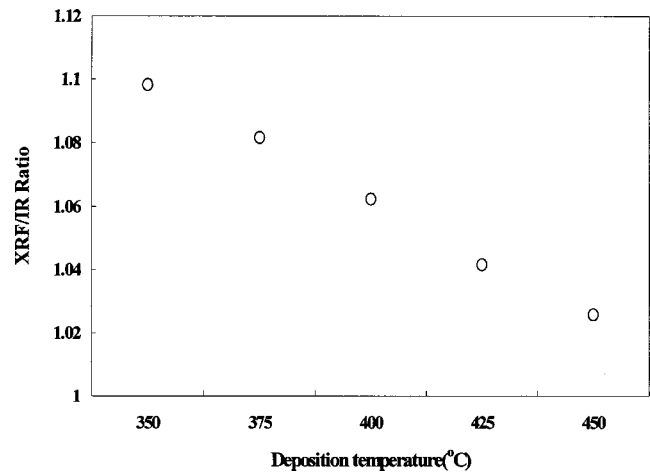


Fig. 5. XRF/Fourier transform IR ratio of SiOF films with varying deposition temperature.

ratio (SiF<sub>4</sub>/SiH<sub>4</sub>) and, thereby, keep the fluorine concentration stable after heat treatment. It is speculated that more SiF<sub>4</sub> (less SiH<sub>4</sub>) would create a greater F% concentration without being bonded with the Si atom. Of course, lowering the gas ratio might also impact the *k*-lowering property of fluorine. So, a proper balance must be struck. A comprehensive study will be reported in another paper.

The thermal stability of SiOF films is also studied using TDS. Gas desorption from films, especially at a lower temperature, has been a concern for device reliability issues, such as the failure of pressure cooling, thermal cycle, and thermal stress tests. The TDS spectra with respect to the mass fragment 18*M/e*, 19*M/e*, and 20*M/e* for SiOF films with different deposition temperatures are checked (not shown). Corresponding to these masses, H<sub>2</sub>O, F, and HF desorption from SiOF films at a lower temperature for a lower deposition temperature are summarized in Table III. As shown, the desorption temperature of Ar is relatively insensitive to the SiOF film deposition temperature. On the other hand, the desorption temperatures of H<sub>2</sub>O, F, and HF are strongly dependent upon the deposition temperature. Higher-deposition-temperature SiOF films have a higher desorption temperature and a lower-desorption pressure. A higher onset of the evolution of desorption temperature means that the film has greater thermal stability during postthermal pro-

TABLE III. TDS analysis for SiOF films with varying deposition temperatures.

Deposition temperature (°C)	350	400	425	450
Ar onset of evolution (°C)	450	455	445	467
Ar peak pressure (10 <sup>-7</sup> Torr)	0.1	0.1	0.1	0.1
H <sub>2</sub> O onset of evolution (°C)	452	467	467	520
H <sub>2</sub> O peak pressure (10 <sup>-7</sup> Torr)	1.0	1.0	1.0	0.5
F onset of evolution (°C)	435	450	467	490
F peak pressure (10 <sup>-7</sup> Torr)	1.0	1.0	1.0	0.5
HF onset of evolution (°C)	410	420	450	467
HF peak pressure (10 <sup>-7</sup> Torr)	1.0	1.0	1.0	0.5

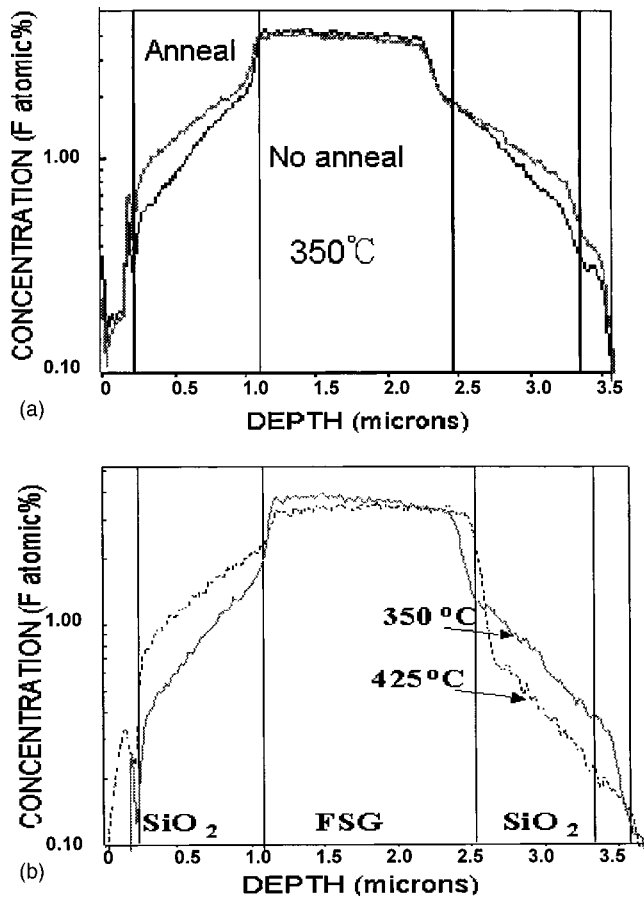


FIG. 6. SIMS profile of SiOF film: (a) Annealing effect (deposition temperature = 350 °C) and (b) deposition temperature effect.

cesses. Consequently, we have demonstrated that SiOF films with a higher-deposition temperature have less moisture content, greater thermal stability, and better suitability for the IMD application in the back-end process.

#### D. Fluorine stability-diffusion issues

Fluorine stability with respect to diffusion within SiOF films strongly influences its utility in IMD integration, with Al wiring delamination as one important area of concern. Fluorine stability was investigated by SIMS using a sandwich structure, consisting of oxide/SiOF/oxide, where the oxides are 2000 Å of SiO<sub>2</sub>. This sandwich structure was deposited on the Si substrate. All samples were annealed at 425 °C for 1 h in a N<sub>2</sub> atmosphere. The annealing test was performed seven times.

As observed in Fig. 6(a), when the SiOF film underwent one thermal treatment, the fluorine atoms diffused into the adjacent oxide films. However, this diffusion was rather modest and the fluorine profile remained quite sharp at the SiOF/SiO<sub>2</sub> interface. Therefore, we concluded that the driving force of fluorine diffusion is the overall thermal budget. Figure 6(b) compares the effect of deposition temperature for fluorine diffusion stability. It shows that the SiOF film with a lower-deposition temperature (350 °C) exhibits a higher fluorine diffusion capability. This is the same data shown in Fig.

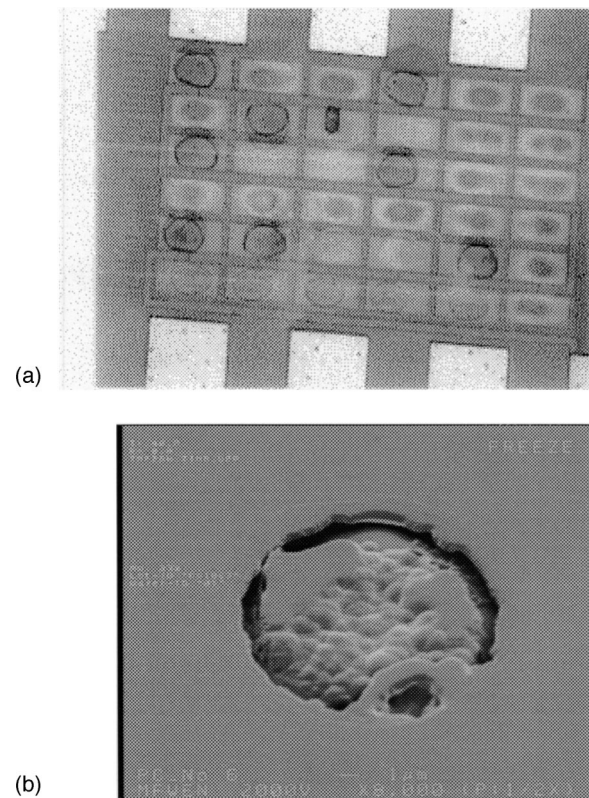


FIG. 7. Integration problems of SiOF film with 350 °C deposition temperature: (a) Optical microscope image of bubble defect on Al pad and (b) SEM image of film peeling.

6(a). The fluorine diffusion length for the SiOF film at 350 °C deposition temperature is about ~500 Å, higher than that (~200 Å) of the SiOF film at 450 °C deposition temperature. Most of the diffused F is believed to originate as weak bonding Si—F or from free fluorine. As a consequence, a lower deposition temperature of the SiOF film causes weaker Si—F bonds to break and diffuse, along with the free fluorine, affecting the stability of the film.

#### E. Interconnect pattern wafer test

The thermal stability of SiOF films with varying deposition temperature is also confirmed using actual Al interconnect test structures. The effect of the deposition temperature on via resistance for the design rule (0.23 width/0.21 μm spacing) of 0.18 μm using SiOF films as an IMD was also checked. Via resistance has no significant difference in any deposition temperature, ranging from 350 to 450 °C (not shown). This implies that SiOF films with a deposition temperature from 350 to 450 °C can be well integrated with a photo and etch process. On the other hand, reliability and defects were frequently detected on patterned wafers, especially in the case of lower-deposition temperatures (350 to 400 °C). A serious bubble defect was observed after completing a seven-layer metal structure. This type of defect was found on the metal pads, shown in Fig. 7(a), similar to the result of Kawashima *et al.*<sup>14</sup> These defects arise from the diffusion of unstable fluorine and the reactions with the un-

derlayer barrier layer (TiN), metal lines (Al), and passivation layer ( $\text{Si}_3\text{N}_4$ ). Another defect type, i.e., peeling, is also observed for a 350 °C SiOF film, as shown in Fig. 7(b). Peeling is hardly ever found in higher-deposition-temperature SiOF films. Additionally, it always occurred after the CMP process. A lower hardness of the SiOF film with a lower-deposition temperature was suspected because the high downforce of the CMP process. To solve these problems of a lower-temperature SiOF film, one should increase the liner and capped layer thicknesses and reduce the downforce in the CMP process. However, a sacrifice of the effective dielectric constant and CMP planarization properties may occur.

#### IV. CONCLUSIONS

The thermal stability for SiOF deposited by HDS-CVD is highly influenced by deposition temperature. All analyses, including SIMS, TDS, and annealing thermal tests, have shown that SiOF films deposited above 400 °C have better thermal stability. However, the high deposition temperature (over 450 °C) creates metal (AlCu) extrusion and melting issues. Patterned wafers with short-loop results have also demonstrated that low-deposition temperature results in F-bubble formation because of greater amount of free fluorine. The results of this study demonstrate that the deposition temperature of SiOF films is extremely important for the thermal stability of the film.

#### ACKNOWLEDGMENTS

Technical support from the Failure Analysis Laboratory of the Taiwan Semiconductor Manufacturing Company (TSMC) is acknowledged. Special thanks are also due to Andy Chen and M. H. Yoo of TSMC for their full support.

- <sup>1</sup>J. Pellerin, R. Fox, and H. M. Ho, *Mater. Res. Soc. Symp. Proc.* **476**, 113 (1997).
- <sup>2</sup>J. A. Theil, F. Mertz, M. Yairi, K. Seaward, G. Ray, and G. Kooi, *Mater. Res. Soc. Symp. Proc.* **476**, 31 (1997).
- <sup>3</sup>H. Yang and G. Lucovsky, *Mater. Res. Soc. Symp. Proc.* **476**, 273 (1997).
- <sup>4</sup>L. Baul, G. Passemar, Y. Gobil, H. M'saad, A. Corte, F. Pires, P. Fugier, P. Noel, P. Rabinzohn, and I. Beinglass, *Microelectron. Eng.* **37**, 261 (1997).
- <sup>5</sup>P. W. Lee, S. Mizuno, A. Verma, H. Tran, and B. Nguyen, *J. Electrochem. Soc.* **143**, 2015 (1996).
- <sup>6</sup>W. Chang, S. M. Jang, C. H. Yu, S. C. Sun, and M. S. Liang, *IEEE (1999) IITC 99-131*.
- <sup>7</sup>H. J. Shin, S. J. Kim, B. J. Kim, H. K. Kang, and M. Y. Lee, *IEEE (1998) IITC98-211*.
- <sup>8</sup>H. M. Baad, *Proceedings of 1999 DUMIC Conference*.
- <sup>9</sup>T. Tamura, J. Saki, Y. Inoue, M. Satoh, and H. Youshitaka, *Jpn. J. Appl. Phys., Part 1* **37**, 2411 (1988).
- <sup>10</sup>C. F. Yeh, Y. C. Lee, K. H. Wu, Y. C. Su, and S. C. Lee, *J. Electrochem. Soc.* **147**, 330 (2000).
- <sup>11</sup>S. Agraharam, D. W. Hess, P. A. Kohl, and S. B. Allen, *J. Electrochem. Soc.* **147**, 2665 (2000).
- <sup>12</sup>S. Lee and J. W. Park, *J. Vac. Sci. Technol. A* **17**, 458 (1999).
- <sup>13</sup>T. Homma, *Thin Solid Films* **278**, 28 (1996).
- <sup>14</sup>Y. Kawashima, T. Ichikawa, N. Nakamura, S. Obata, Y. Den, H. Kawano, T. Ide, and M. Kudo, *IEEE Trans. Semicond. Manuf.* **12**, 302 (1999).